

3次元組織作製に向けた細胞用インクジェット技術の開発

High-precision Three-dimensional Inkjet Technology for Live Cell Bioprinting

松本 貴彦* 高木 大輔* 林 和花* 柳沼 秀和* 邊見 奈津子*
 Takahiko MATSUMOTO Daisuke TAKAGI Waka LIN Hidekazu YAGINUMA Natsuko HEMMI

旗田 茂雄* 瀬尾 学*
 Shigeo HATADA Manabu SEO

要 旨

近年、再生医療用途や創薬開発向けにin vitroで3次元組織体を構築する技術が求められており、その1つとしてバイオプリント技術が有望視されている。我々は、3次元組織体構築に向け複数種類の細胞や積層材料を精密に配置できるバイオプリントシステムを開発した。細胞吐出させるために新規に開発したインクジェットヘッドは細胞を生きたまま吐出可能であり、かつピエゾ素子でメンブレンを振動させて細胞液を攪拌することでノズル閉塞を回避できるため、安定的なオンデマンド吐出が可能である。本インクジェット技術を搭載したバイオプリントシステムにより、吐出細胞数の制御や細胞の2次元配置を達成すると共に、ハイドロゲルと細胞それぞれの層を交互に積層することでミルフィーユ状の3次元構造体構築プロセスを提案した。本バイオプリントシステムは既往の技術を凌駕するレベルでの細胞プリントを達成し得るものと期待できる。

ABSTRACT

In recent years, bioprinting has emerged as a promising technology for the construction of three-dimensional (3D) tissues to be used in regenerative medicine or *in vitro* screening applications. In the present study, we report the development of an inkjet-based bioprinting system to arrange multiple cells and materials precisely into structurally organized constructs. A novel inkjet printhead has been specially designed for live cell ejection. Droplet formation is powered by piezoelectric membrane vibrations coupled with mixing movements to prevent cell sedimentation at the nozzle. Stable drop-on-demand dispensing and cell viability were confirmed over a long enough time to allow the fabrication of 3D tissues. Reliable control of cell number and spatial positioning was demonstrated using two separate suspensions with different cell types printed sequentially. Finally, a process for constructing stratified Mille-Feuille-like 3D structures is proposed that alternately superimposes cell suspensions and hydrogel layers with a controlled vertical resolution. Experimental results show that our inkjet technology is effective for both two-dimensional patterning and 3D multilayering and has the potential to facilitate the achievement of live cell bioprinting with an unprecedented level of precision.

* HC事業本部 バイオメディカル事業センター
 Biomedical Business Center, Healthcare Business Group

本稿は、Whoice Publishing Pte. Ltd.より著作権の利用許諾を受け、*International Journal of Bioprinting*, Vol. 5, Issue 2 (2019)に掲載した論文を基に作成した。

1. Introduction

The field of tissue engineering has developed considerably in recent years, along with the increasing interest in regenerative medicine globally. Advances in stem cell research, particularly the discovery of induced pluripotent stem cells¹⁾, have provided a means to culture and manipulate cells from organs, which were once considered impossible to regenerate. *In vitro* production of functional tissue analogs has become a reality, and tissue engineering has numerous potential applications in therapeutic areas including tissue repair and organ replacement, in addition to the development of applications to drug discovery, disease modeling, and alternatives for animal testing. Today, one of the major challenges is how to reproduce three-dimensional (3D) structures of tissues with matching complexity and functionality. The development of novel technologies for biofabrication, particularly bioprinting, has attracted a lot of attention considering their potential to arrange cells and materials into structurally organized constructs²⁾.

Current bioprinting technologies are based on three major approaches comprising inkjet, extrusion, and laser printing methods^{3,4)}. Extrusion-based strategies are the most extensively developed due to their capacity to develop 3D constructs and networks in a relatively straightforward manner using high viscosity materials that can integrate extracellular matrix (ECM) such as collagen. However, this approach is not suitable for our purposes since it does not facilitate precise control over the deposition of a small number of cells. Although lasers facilitate printing with a very high resolution, the productivity remains limited due to the complexity and cost of the system, in addition to requirements relating to the preparation of the ribbons of cells and hydrogels. In contrast, inkjet printing, and more generally, droplet-based bioprinting⁵⁾, have great promise as a simple and efficient method for the precise patterning of multiple cell types and bioink components such as active

biomacromolecules⁶⁾, especially since a drop-on-demand control of small volumes down to a few hundred picoliters can be expected. However, inkjet technology has several limitations that impair its further adoption in 3D construction. Although some of the earliest reports of successful bioprinting in the mid-2000s were inkjet based⁷⁻⁹⁾, few concrete results of fully functional inkjet-produced tissues have been reported to date.

The first notable limitation of inkjet bioprinting is that ejecting large cell-sized particles from common printheads is difficult. While successful ejection has been reported¹⁰⁻¹³⁾, and acoustic ejection has been achieved in live cell printing¹³⁾; cell sedimentation inside the printhead chamber and clogging of the nozzle are expected to rapidly compromise any reliable control of droplet formation over the length of time required to produce a 3D tissue. Second, the range of materials that can be used as substrates to carry the cells is limited to ejectable low viscosity liquids, so shaping fine 3D structures with suitable mechanical properties is particularly challenging. Various strategies have been proposed to combat this, including coprinting hydrogel precursors with the appropriate cross-linking agent, which facilitates rapid gelation on contact¹⁴⁻¹⁶⁾ or deposition of one liquid into a bath of the other one¹⁷⁾. However, so far, the results have been generally limited to two-dimensional (2D) cell patterning or roughly shaped 3D cell-laden structures with no spatial positioning at the cellular level.

To address the above challenges, we report here the development of an inkjet bioprinter equipped with a newly designed printhead specially optimized for live cell ejection. For this purpose, we have adapted a bending-type piezoelectric actuator coupled to a simple open head chamber without any narrow flow channel. Such a piezoelectric device has been applied in some previous publications from other groups for continuous cell spraying, but very few studies have reported its application to drop-on-demand cell deposition¹⁸⁾. The present study integrates the droplet formation and mixing

mechanism in our prototype printhead. The stability of cell dispensing and viability is validated over an adequately extended period to facilitate the fabrication of a substantial tissue construct. We then demonstrate the feasibility of building a multi-ink printing system to construct stratified Mille-Feuille-like structures with controlled thickness by alternating cell suspension and hydrogel layers. Therefore, exploiting the full potential of inkjet technology promises to facilitate high-precision multi-ink 3D bioprinting.

2. Materials and Methods

2-1 Cell Cultures

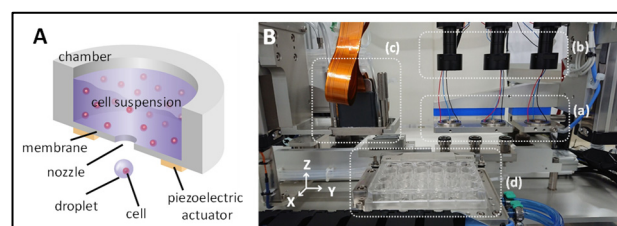
All cells were cultured in a 5% CO₂ incubator at 37.0°C and passaged manually every 2 to 3 days to maintain a subconfluent state. NIH/3T3 mouse fibroblast cell line (clone 5611, JCRB Cell Bank) and normal human dermal fibroblasts (NHDF, CC-2509, Lonza Inc.) were cultured in Dulbecco's Modified Eagle's Medium (Thermo Fisher Scientific Inc.) supplemented with 10% fetal bovine serum (Biowest) and 1% penicillin-streptomycin (26253-84, NACALAI TESQUE, INC). Human umbilical blood vein endothelial cells (HUVEC, CC-2519, Lonza Inc.) were cultured in an endothelial cell growth medium (EGM, Lonza Inc.) with supplements as recommended by the manufacturer. For bioink preparation, the cells were washed twice with Dulbecco's phosphate-buffered saline without calcium and magnesium (DPBS, Thermo Fisher Scientific Inc.), detached with 0.05% Trypsin-EDTA (25300054, Thermo Fisher Scientific Inc.), and centrifuged at 400 g for 5 min at 4°C. The cell pellets were re-suspended in fresh DPBS at room temperature and used within 30 min after suspension.

2-2 Inkjet Print Head Development

The cell-printing head in Fig. 1A presents an original architecture comprising a chamber holding the cell

suspension, a disk membrane (which is fixed at the circumference of the bottom of the chamber), a nozzle with an aperture at the center of the membrane, and an annular piezoelectric actuator fixed outside below the membrane

We were able to perform subsequent experiments with more advanced processes for the spatial positioning of cell-containing droplets by achieving a reliable ejection of living cells.



(A) Schematic cross-sectional 3D view of the cell-printing head. (B) Photograph of the 3D bioprinting system setup composed of (a) three cell-printing heads controlled in the X and Z directions, (b) cameras for real-time observation of the mixing state in the inkjet head chambers, (c) two industrial inkjet heads for hydrogel printing controlled in the same directions as (a), and (d) a plate/slide holding stage controlled in the Y direction.

Fig. 1 Overview of the inkjet bioprinting system.

2-3 Evaluation of Inkjetting Condition

To determine the optimal printing conditions, optical monitoring devices were assembled as follows. Observation of drop formation was carried out with an experimental apparatus featuring a high-speed camera (HPV-2, Shimadzu Corporation) and a stroboscopic flash lamp (PE60-SG, Panasonic) aligned on a horizontal axis under the printhead nozzle. The chamber was filled with NIH/3T3 suspension with DPBS solution. By applying a signal to the piezoelectric actuator of the cell-printing head, a droplet is ejected from the cell-printing head. The frequency of the applied signal was fixed to the fundamental frequency of the membrane.

2-4 Evaluation of Mixing Condition

Observation of cell suspension mixing was carried out with an experimental apparatus featuring a ring-type

illumination source, a macro zoom lens (TS-93005, SUGITOH), and a CCD image sensor (DFK23U618, Imaging Source) placed above the print head chamber. The chamber was filled with 3T3 suspension with DPBS solution, and the signal with several frequency components was applied to the piezoelectric actuator for observation.

2-5 Evaluation of Cell Ejection Stability

To evaluate ejection stability, NIH/3T3 cell suspensions were fluorescently labeled with Cell Tracker Green (Thermo Fisher Scientific Inc.) and diluted in DPBS at determined densities before being loaded into the inkjet printhead chamber. Ejecting mode signals and mixing mode signals as defined above were applied alternately at intervals of 500 ms, which allowed the deposition of droplets at a frequency of 2 Hz. The droplets were deposited onto glass slides fixed to an automated moving stage so that the number of cells in each droplet could be counted after printing under a fluorescence microscope (Axio observer D1, Carl Zeiss).

2-6 Cell Viability Assay After Ejection

NIH/3T3 or HUVEC cell suspensions were prepared at concentrations of 1×10^6 cells/ml in DPBS. Thirty μL of the cell suspension was loaded into the inkjet head chamber. The cells were ejected for about 30 min with a droplet ejection frequency of 100 Hz into a microcentrifuge tube containing 1 ml of the appropriate culture medium and then counted and dispensed into a 96-well culture plate at a density of 3×10^3 cells/well. Cell ejection experiments were conducted in triplicate. As control samples, the initial cell suspensions before ejection were manually dispensed into a 96-well culture plate using a 100 μL micropipette. The plates were placed in a 5% CO₂ incubator at 37.0°C until measurement. Apoptotic and necrotic cells were quantified in each well using the Apoptotic/Necrotic cell detection kit (Promokine, PromoCell GmbH) according to the

instructions of the manufacturer. The stained cultures were observed under a fluorescence microscope (Axio observer D1, Carl Zeiss), and images were taken so that between 200 and 500 cells could be analyzed for each sample. Early apoptotic cells were identified on the basis of green fluorescent staining (FITC-Annexin V) of their plasma membranes and necrotic cells on the basis of red fluorescent staining (EthD-III) of their nuclei. Double positive cells exhibiting both green and red fluorescent staining were considered late apoptotic cells. The total number of cells was determined by counting all the nuclei stained in blue by Hoechst 33342.

2-7 Cell Proliferation Assay

The cell suspensions were ejected into a microcentrifuge tube for the cell viability assay and dispensed into a 96-well culture plate at a density of 3×10^3 cells/well. The WST-1 colorimetric assay (Premix WST-1 Cell Proliferation Assay System, Takara Bio Inc.) was used to evaluate the proportion of actively metabolizing live cells in each well. Measurements were performed in triplicate using three wells at each time point. Ten μL of the WST-1 reaction solution was added to each well containing the cells and 100 μL culture medium. The plates were returned to the 5% CO₂ incubator for 1 h and incubated at 37.0°C. Absorbance at 420 nm was measured using a plate reader (Cytation 5, BioTek Instruments, Inc.). The measured data were normalized relative to the measurements obtained 4 h post-ejection.

2-8 Embryonic Stem Cell Clonogenic Assay and Immunostaining

Mouse embryonic stem cells (mES cells, Merck) were maintained in gelatin-coated dishes with feeder cells (Merck) as recommended by the manufacturer. The cells were detached using Accutase (Merck), centrifuged at 100 g for 5 min at 4°C, and suspended in DPBS through a 20 mm filter to make bioinks. After ejection, the cells were seeded at a density of 2.5×10^4 cells/well in 24-well plates

and cultured for 3 days. The average numbers of colony-forming units were counted after staining with a red alkaline phosphatase substrate kit (VECTOR Laboratories). For immunostaining, the cells were fixed with 4% paraformaldehyde and incubated overnight at 4°C with primary antibodies, Nanog (abcam) 1:200, SSEA-1 (abcam) 1:100, 2 h at room temperature with secondary antibodies, and 5 min with 1:10,000 Hoechst 33342 (Thermo Fisher Scientific).

2-9 3D Bioprinting System Setup

We designed a bioprinting system (Fig. 1B) for constructing 3D tissues with multiple cell types. The present system is equipped with newly developed cell-printing inkjet heads and commercial industrial inkjet heads for ejecting biomaterials. A maximum of three cell-printing inkjet heads can be mounted in parallel so that three types of cells can be printed sequentially to develop tissues with heterogeneous patterns. The position of the nozzle is controlled horizontally on the X-axis and vertically on the Z-axis to allow the deposition of cells not only for surface patterning but also in three dimensions. In addition, two industrial multi-nozzle inkjet heads (MH2420 Print Head, Ricoh) allow the successive printing of two different liquids such as a hydrogel precursor and an appropriate cross-linking reagent, enabling the formation of fast-gelling layers over a large area. The industrial heads can also be controlled independently on the X- and Z-axis. The stage is controlled on the Y-axis and can hold glass slides at the back and culture plates at the front.

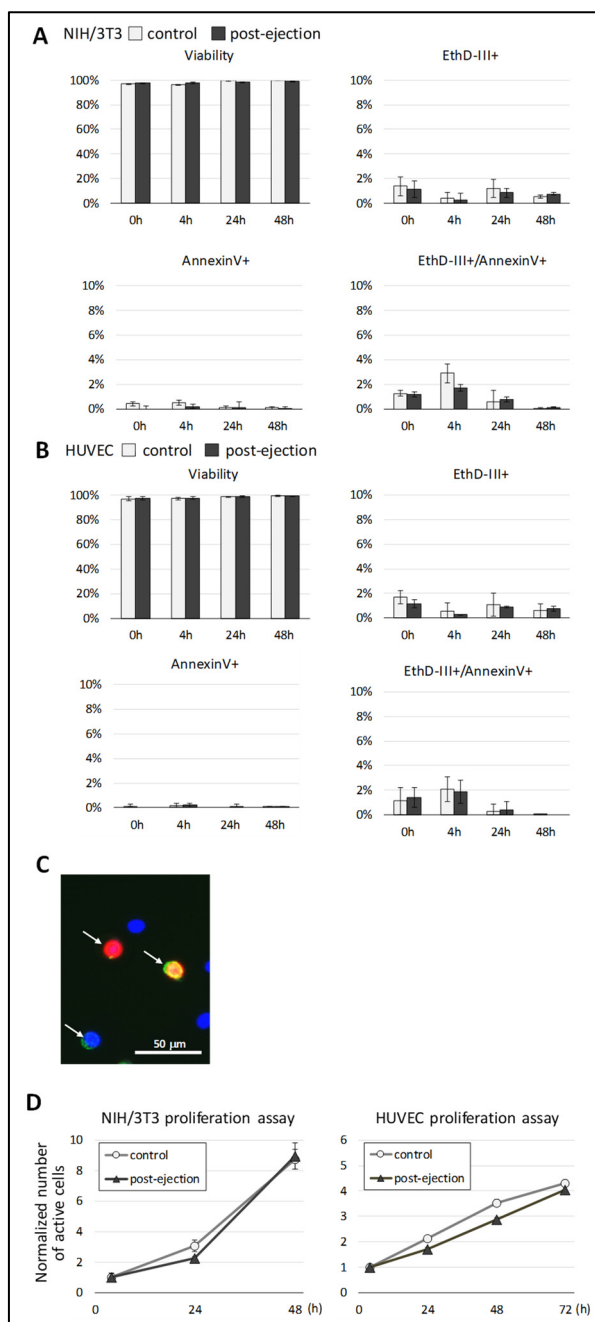
2-10 2D Drop-on-demand Patterning Evaluation

To evaluate the control of droplet deposition using two cell-printing heads in a sequential manner, two separate suspensions of NIH/3T3 cells were prepared at a concentration of 3×10^6 cells/ml in DPBS. To distinguish between the suspensions, the cells were fluorescently labeled with CellTracker Green or Orange (Thermo Fisher

Scientific Inc.) according to the instructions of the manufacturer. Cell-containing droplets were deposited with a sinusoidal waveform and an ejection frequency of 50 Hz onto a glass slide. Phase-contrast and fluorescent microscopy images were taken using a laser scanning confocal microscope (FV10i, Olympus Corporation).

2-11 3D Multilayering Evaluation

For 3D constructs, the general process for developing multilayered structures with alternating cell and hydrogel deposition is depicted in Fig. 2. Four separate bioinks were prepared as follows: 0.5 wt% sodium alginate as scaffold bioink 1; 100 mM calcium chloride (CaCl₂) as scaffold bioink 2; 5×10^7 cells/ml NHDF cells stained with Cell Tracker Green and suspended in DPBS and 0.5 wt% sodium alginate as cell-laden bioink 1; and 5×10^7 cells/ml NHDF cells stained with Cell Tracker Orange and suspended in DPBS and 0.5 wt% sodium alginate as cell-laden bioink 2. Printing was performed on a glass slide as follows: (a) A layer of sodium alginate was deposited by ejecting scaffold bioink 1 using the first industrial head at 10 Hz, immediately followed by (b) a layer of CaCl₂ using the second industrial head for rapid gelling of a thin alginate hydrogel scaffold layer; (c) Cell-laden bioink 1 was deposited with a cell-printing printhead at 10 Hz to draw a 10 mm line along the X-axis; (d) a hydrogel scaffold layer was superimposed onto the cell layer using the same procedure in (a) and (b); and (e) the cell-laden bioink 2 was deposited with a cell-printing printhead at 10 Hz to draw a 10-mm line along the Y-axis. Steps (a)-(e) were repeated until a 10-layer construct was formed. To observe the superposition of layers, cross-sectional Z-stack images of the multilayered constructs were acquired using a confocal laser scanning microscope (TCS SP8 STED CW, Leica Microsystems) at the intersection of the green and orange cell lines after fixation in ethanol.



(A) Percentages of unstained viable cells, EthD-III positive (necrotic) cells, FITC-Annexin V positive (apoptotic) cells, and double positive (late apoptotic) cells in NIH/3T3 cell cultures from 0 to 48 h post-ejection compared with control cultures seeded by manual pipetting. Error bars show the standard deviations of triplicate cultures with 200 to 500 cells analyzed per sample. (B) Same as (A) for HUVEC cultures. (C) Representative fluorescence microscopy image of NIH/3T3 cells stained using the Apoptotic/Necrotic cell detection kit. White arrows indicate the three different types of stained cells: red cells for EthD-III, green cells for FITC-Annexin V, and double positive yellow cells. All cell nuclei are stained blue with Hoechst 33342. Scale bar: 50 μ m. (D) Quantification of active live cells in NIH/3T3 and HUVEC in WST-1 proliferation assay. The data were normalized and reported as a ratio relative to the measurement at 4 h.

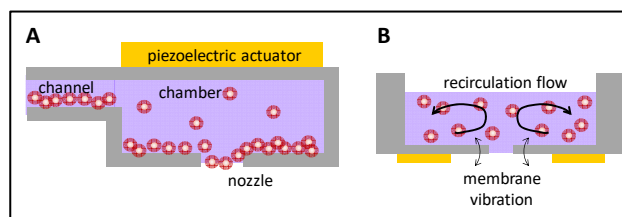
Fig. 2 Analysis of cell survival after ejection from the new inkjet head.

3. Results

3-1 Inkjet Printhead Design

Ejecting living cell suspensions using inkjet technology generally presents several challenges. Figure 3A shows a simplified representation of a common piezoelectric inkjet printhead and summarizes the three most notable issues when using such a device. First, as the typical cell size is 100 times larger than typical pigments in printing ink solutions, nozzle and channel clogging occurs as cells rapidly sink to the bottom. Cell sedimentation also makes it a challenge to obtain a stable number of cells per droplet since the density inside the chamber is not maintained at a homogeneous state. Second, air bubbles are trapped in the cell suspension due to high surface tension, which negatively affects the reliability of droplet ejection. Third, a cell suspension with a large volume is required to fill up the entire chamber and enable the piezoelectric actuator to induce liquid pressure for droplet ejection.

To combat these issues, we have developed a novel printhead optimized for live cell-printing (cell-printing head) that could replace conventional printheads. As shown in Fig. 3B, the cell-printing head is composed of an open chamber where the cells are directly loaded, a disc-shaped membrane fixed at the circumference of the bottom of the chamber, a nozzle with an aperture at the center of the membrane, and an annular piezoelectric actuator fixed on the outer side of the membrane. The advantages of the cell-printing head are that first, as illustrated in Fig. 3B, membrane movements driven by the piezoelectric actuator can establish a recirculating flow inside the chamber to prevent cell sedimentation. Second, air bubbles trapped during droplet ejection can be easily evacuated from the open side. Third, the cell-printing head can be loaded with volumes as low as a few dozen microliters without compromising droplet formation.



(A) Common printhead showing nozzle clogging with sedimentation of cells. (B) Cell-printing head, with a recirculation flow generated by membrane vibration to prevent nozzle clogging.

Fig. 3 Schematic diagram of a cross-sectional view of inkjet heads.

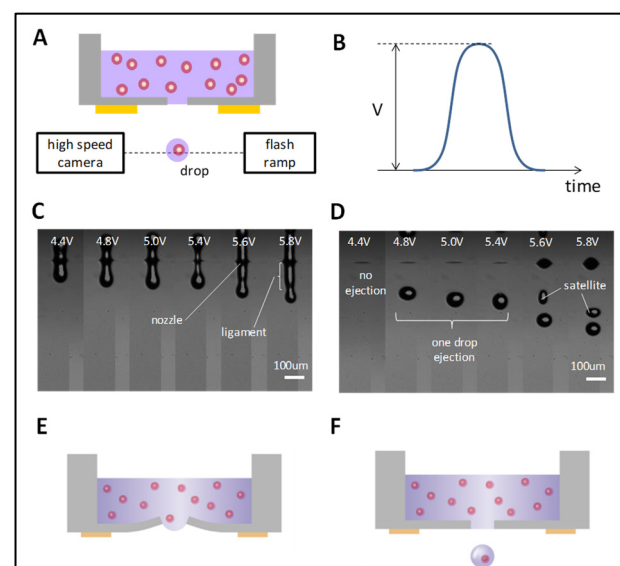
3-2 Evaluation of Inkjetting Condition

To determine the optimal printing conditions, optical monitoring devices were assembled as follows. Observation of drop formation was carried out, as illustrated in Fig. 4A. By applying a signal (Fig. 4B) to the piezoelectric actuator of the cell-printing head, a droplet is ejected from the cell-printing head. The frequency of the applied signal was fixed to the fundamental frequency of the membrane.

Results of drop formation with voltage amplitudes between 4.4 and 5.8 V are shown in Fig. 4C. One drop formation is achieved when the voltage ranges from 4.8 to 5.4 V. When the voltage is lower than 4.8 V, the pressure required for drop formation cannot be achieved. Conversely, when the voltage is higher than 5.4 V, minute droplets (mist and satellite) are formed.

Next, we describe a droplet forming process in the cell printhead with reference to the schematic view in Fig. 4E and F. When the membrane is displaced from the original state to the liquid chamber side and suddenly pushes the liquid; pressure is generated at the interface between the membrane and liquid. Since the pressure is easily released into the atmosphere through the nozzle rather than through the upper aperture of the chamber or pushes back the membrane, the meniscus protrudes out of the nozzle (Fig. 4E). Thereafter, the membrane attempts to revert to the original position. However, if the liquid in the nozzle portion at the time receives an adequate velocity, the

liquid droplet is considered to be formed, as shown in Fig. 4F.



(A) Observing mechanism of droplet formation using a high-speed camera and a flash lamp. (B) Addition of sine curve signals to piezoelectric actuator. (C) Observation of droplet after 200 μ s with additions of 4.4, 4.8, 5.0, 5.4, 5.6, and 5.8 V to compare each droplet formation. (D) Observation of droplet after 316 μ s and one drop ejection with 4.8, 5.0, and 5.4 V. (E) Schematic diagram of droplet formation in 200 μ s. (F) Schematic diagram of droplet forming in 316 μ s.

Fig. 4 Observation of droplet formation from the cell printhead.

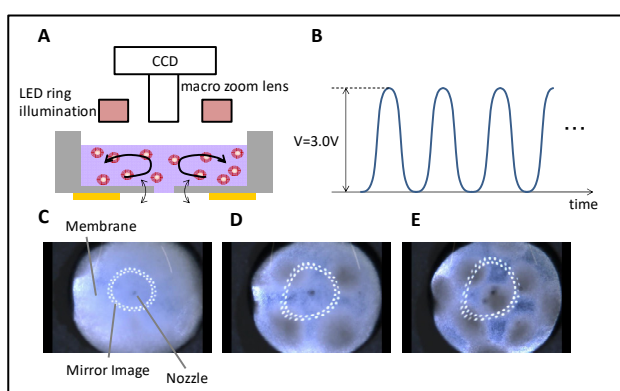
3-3 Evaluation of Mixing Condition

Observation of cell suspension mixing was carried out as illustrated in Fig. 5A, and the signal is shown in Fig. 5B with several frequencies applied to the piezoelectric actuator for the observation.

The circle in each figure indicates the membrane. The nozzle is located in the center of the membrane, and ring-shaped mirror images of the illuminations are visible in each figure. In Fig. 5C, uniform mixing mode is observed by applying the signal at a frequency near the fundamental frequency of the membrane (20 kHz). Conversely, the periodic pattern is observed by applying a higher frequency such as 72.0 kHz. In Fig. 5D and E, 74.0 kHz is applied. The phenomena are expected to induce higher-order vibration modes. At such a higher-order vibration mode, the antinodes and nodes of vibration are generated, and cells gathering into the node position are observed, as

shown in Fig. 5D and E. Therefore, the preferred signal frequency for mixing cells is not one of a higher-order vibration mode of the membrane but one near the fundamental mode.

Appropriate single cell droplet formation was achieved when a single peak sinusoidal signal was applied to the piezoelectric actuator with a voltage amplitude between 4.8 and 5.4 V (ejecting mode), whereas uniform mixing was achieved when the signal had a frequency close to the fundamental frequency of the vibrating membrane at a fixed amplitude of 3 V (mixing mode).



(A) Mixing status is checked by CCD, a micro zoom lens, and ring illumination. (B) For mixing cell suspension, a sinusoidal signal was applied with a fixed amplitude of 3.0 V. (C) Mixing status with fundamental frequency of the membrane, 20 kHz. (D) and (E) Mixing mode with higher-order vibration mode, 72.0 and 74.0 kHz.

Fig. 5 Observation of mixing cell suspension in the chamber.

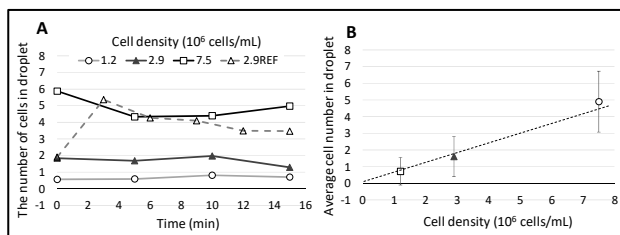
3-4 Evaluation of Ejection Stability

Developing bioprinted tissue at any substantial volume or amount, as required in applications such as organ regeneration or drug screening, would require a reliable deposition of cell-containing droplets over a considerable period. Therefore, maintaining a stable number of cells per droplet for an adequately long time is critical in inkjet bioprinting. Optimization of the signals applied to the piezoelectric actuator to enable the use of the cell-printing head is described in section 2.2. Briefly, a single peak sinusoidal signal with a voltage amplitude between 4.8 and 5.4 V (ejecting mode) allows a single cell-containing

droplet to be ejected by the movement of the membrane at the nozzle. Drop-on-demand ejection, therefore, can be achieved by controlling the signal applied to the printhead. Between each ejection, a weak sinusoidal vibration is applied to the membrane to maintain the cells in suspension (mixing mode). Alternating the ejecting mode and mixing mode signals at fixed time intervals allows the deposition of droplets at a constant frequency. The results for the evaluation of ejection stability are shown in Fig. 6A. Droplets were ejected at a frequency of 2 Hz using cell suspensions at three different cell densities and were ejected without mixing mode as a reference. The number of cells per droplet was stable for over 15 min at all of the tested cell densities with mixing mode. Conversely, unstable ejecting was observed with the reference sample. At 0 min, the same cell number was observed with mixing and without mixing; however, average cell number increased with the lapse of time. The observations indicate that mixing mode could be ejected with stable cell number. The graph in Fig. 6B illustrates the average cell number and the standard deviation with mixing mode samples calculated over the entire length of the 15 min ejection experiment. The average number of cells per droplet had a linear relationship with the initial density of cell suspension, which suggests that the number of cells per droplet can be adjusted by selecting the appropriate cell density when preparing the bioink cell suspension. Here, using a bioink with a cell density of 3×10^6 cells/ml would allow the deposition of around 1.5 cells per droplet on average. This indicates that high accuracy control of cell number in each droplet can be achieved by using the cell-printing head.

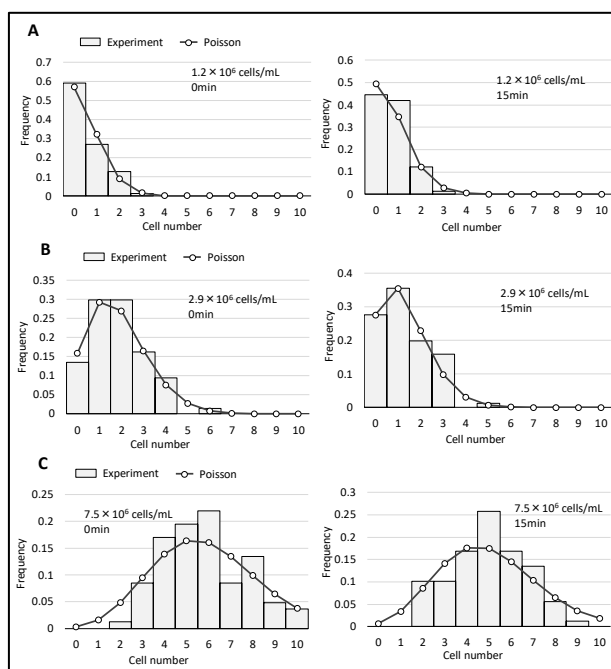
In addition, the histograms in Fig. 7 show that the number of cells per droplet at 0 and 15 min is consistent with a Poisson distribution profile at all of the tested cell densities. The observation indicates that the cells inside the head chamber were maintained in suspension with a random distribution for a long time, which confirms that

the mixing mode of the cell-printing head achieved its function.



Droplets of cell suspensions were ejected at a frequency of 2 Hz onto a glass slide. Then, the cell number in each droplet was counted under a fluorescence microscope. (A) Average cell count per droplet for three initial cell densities: 1.2×10^6 , 2.9×10^6 , and 7.5×10^6 cells/mL. As a reference, 2.9×10^6 cells/mL were ejected without mixing mode. (B) Average cell number in droplet are plotted with each cell density. Error bar is standard deviation.

Fig. 6 Evaluation of ejection stability.



(A) Result with 1.2×10^6 cells/mL in 0 and 15 min. Dot is value with Poisson distribution. Blue bar is experimental value. (B) Result with 2.9×10^6 cells/mL. (C) Result with 7.5×10^6 cells/mL.

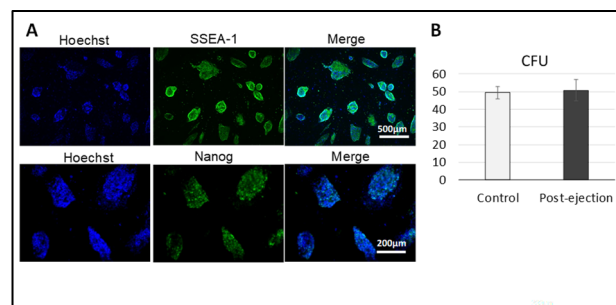
Fig. 7 Histogram plot of cell number in each droplet.

3-5 Cell Viability and Proliferation after Ejection

Cell viability was evaluated at 0, 4, 24, and 48 h after ejection into the culture medium. Printing was carried out with the voltage previously applied but with the droplet ejection frequency increased to 100 Hz to enable the collecting of a higher number of cells. The cells were

ejected into the culture medium for 30 min and then aliquoted into a 96-well plate and placed in a 5% CO₂ incubator at 37.0°C. The cultures were then fluorescently stained with FITC-Annexin V to identify early apoptotic cells in green and with Ethidium Homodimer III (EthD-III) to identify necrotic cells in red. The percentages of each cell type relative to the total number of cells analyzed post-ejection were compared with those of control cultures seeded by manual pipetting.

As shown in Fig. 2, very high viability of between 97% and 99% was demonstrated for NIH/3T3 and HUVEC after printing. No significant difference was observed compared with the control cultures, either for apoptotic cells or necrotic cells. The WST-1 proliferation assay revealed that despite a slight decrease at 24 h in NIH/3T3 cells and between 24 and 48 h for HUVEC, the post-ejection samples recovered normally and achieved a proliferation rate similar to that of the manually seeded controls after 48–72 h. To further assess functional recovery in a more sensitive type of cells, a similar experiment was performed using mES cells, as shown in Fig. 8. No significant effect was observed on the clonogenic ability and the expression of stem cell markers in mES cells cultured for 3 days after ejection. Overall, the results demonstrate that using our newly developed inkjet printhead does not significantly affect cell viability and functionality, at least for the cell types used in the present study.



(A) Immunostaining of mES colonies with stem cell markers. (B) Average number of CFU counted at day three of culture after seeding by manual pipetting (control) or by inkjet (post-ejection). Error bars show the standard deviations of four microscopic images.

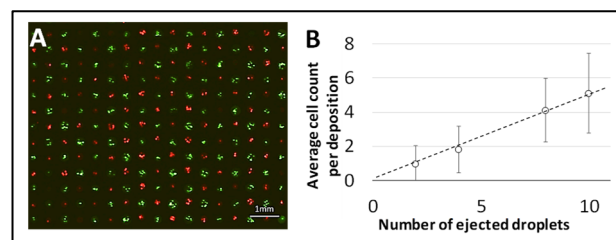
Fig. 8 Analysis of mES cell clonogenic cell survival.

3-6 Precise Drop-on-demand Live Cell Patterning

We developed a novel inkjet bioprinting system (Fig. 1B) to demonstrate the feasibility of multi-ink live cell deposition. Our bioprinter is equipped with three of the novel cell-printing heads described previously, which allow handling of up to three independent cell suspensions simultaneously.

Drop-on-demand control of cell deposition was evaluated by ejecting a predefined number of droplets of cell suspensions onto a glass slide. Fig. 9A shows the results using two different suspensions of fibroblast cells at a density of 3×10^6 cells/ml, one labeled with fluorescent cell tracker green and the other with cell tracker orange, with a distance of 500 μm between the dots. The previous results for ejection stability showed that when using a suspension with the initial density of 3×10^6 cells/mL, about 1.5 cell count per droplet can be expected on average. Here, two droplets were deposited per dot, which allowed the observation of an average of three cell counts per dot.

We also assessed the ability to control cell number with variable droplets, as shown in Fig. 9B. The average number of cells per deposition exhibited a linear relationship with the number of ejected droplets, which suggests that the number of cells per deposition can be adjusted by selecting the appropriate number of droplets. This indicates that highly accurate control of the cell number in each deposition is also achieved with the cell-printing head.



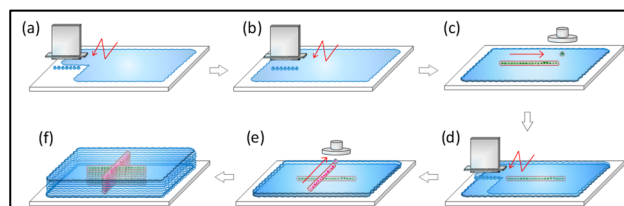
(A) Fluorescence microscope image of green- and red-labeled NIH/3T3 cells deposited alternately at 500 μm intervals with two cell-containing droplets ejected at each position. (B) Ability to control the number of cells based on the number of ejected droplets. Cell ink was formulated to contain one cell in two droplets. Error bars show the standard deviations.

Fig. 9 Drop-on-demand 2D patterning evaluation.

3-7 Biofabrication Process for the Development of 3D Mille-Feuille-like Constructs

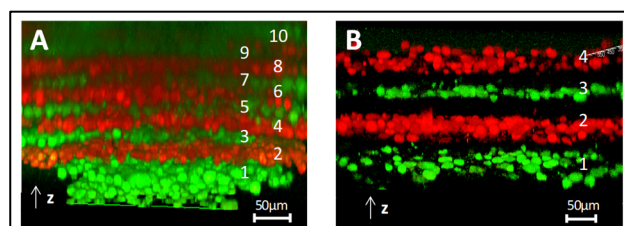
A multilayering process for constructing 3D tissues was developed, as depicted in Fig. 10. In addition to being equipped with cell-printing heads, our inkjet bioprinting prototype has two industrial multi-nozzle heads, which allow rapid deposition of two liquid materials such as precursors of hydrogel scaffolds into thin layers.

By alternating hydrogel scaffold layers made of sodium alginate deposition, followed immediately by CaCl_2 ion cross-linking, and fluorescently labeled cell suspension layers, Mille-Feuille-like bicolor constructs could be produced, as shown in Fig. 11A. Cross-section images along the vertical Z-axis acquired under confocal laser scanning microscopy revealed that the finely stratified multilayer structure was well preserved. As shown in the example in Fig. 11B, we also found that the distance between each cell layer could be controlled by increasing the number of steps during the deposition of the hydrogel scaffold layers.



(a) Printing of a scaffold hydrogel precursor before gelation. (b) Printing of gelation factor. (c) Printing of the first cell ink. (d) A hydrogel scaffold layer is superimposed onto the cell layer by the same procedure in (a) and (b). (e) Printing of the second cell ink. (f) Steps (a)–(e) are repeated until a multilayer construct is achieved.

Fig. 10 Schematic of 3D inkjet cell-printing process.



(A) Ten-layer constructs made by the alternate printing of green and red fluorescently labeled fibroblasts with alginate hydrogel scaffold layers deposited in between. (B) Four-layer constructs with distances between each cell layer increased by the deposition of thicker hydrogel layers.

Fig. 11 Confocal fluorescence microscope Z-stack images of multilayered mille-feuille-like 3D cellular constructs.

4. Discussion

The newly developed inkjet printhead introduced in the present study has been particularly optimized for live cell bioprinting. The unique features of the cell-printing head allow the controlled ejection of single droplets on demand while maintaining the cells in suspension inside the printhead chamber. Our analysis of the number of cells per droplet revealed that a stable ejection could be maintained for dozens of minutes of continuous printing, which is a significant improvement over conventional piezoelectric printheads. Notably, achieving a consistent cell count per droplet and, more preferably, approaching a state where a single cell is contained in each droplet would be a major step toward the modeling of highly detailed 3D structures at the resolution of a single cell. The results showed that the new cell-printing head could eject cells with a cell per droplet consistent with the Poisson distribution profile,

which indicates that the cell suspension was maintained in a well-homogenized state by the mixing system.

However, to achieve an even narrower distribution and further increase the precision of deposition, it would be necessary to bring the state of random distribution closer to a state of uniform distribution for the cells in suspension inside the printhead chamber. This would require a strong repulsive force that acts between the cells, so that they are not brought close to each other, for example, by introducing a polymer with a charge polarity that could provide an electrostatic repulsive force between the cells. We are also investigating the potential of utilizing additional optical cell count systems to further control the number of cells per droplet.

Regarding the suitability of using the new printheads with living cells, analysis of cell viability and proliferation revealed that the ejected cells were not significantly affected, even following the application of sensitive cells such as undifferentiated stem cells. In a previous report evaluating cell injury during laser bioprinting¹⁹⁾, no marked increase in necrotic nor in apoptotic cells was observed from 0 to 48 h. The results are potentially because the level of stress induced by our current process is lower than that in laser printing. The cells recovered and proliferated normally after inkjet printing and were expected to maintain the integrity of their functions, including the clonogenicity of stem cells.

Our printheads bear several features that are considerably different from common industrial inkjet heads and could minimize cell damage. The open chamber structure and the mixing system allow use over extended periods without compromising gaseous exchange, whereas rapidly evacuating bubbles before their accumulation increases the risk of damage following rupture²⁰⁾. The simplicity of the printhead chamber architecture and the use of membrane vibration for droplet generation avert any excessive increase in liquid pressure and shear stress before ejection. Further investigations are

required to assess the physical mechanisms that negatively influence cell viability and function the most.

From a practical point of view, it is also worth noting that, particularly considering potential biomedical applications, the printhead chamber was intentionally kept simple to ensure that low volumes of cell suspensions could be loaded easily. Simplifying the procedures for loading and exchanging cell suspensions could further reduce the risks of environmental stress and contamination. This could also be a major advantage when using rare cells that are difficult to expand since our system does not require filling ink cartridges or wasting cell suspensions for maintenance.

Achieving a reliable ejection of living cells enabled us to subsequently experiment with more advanced processes for the spatial positioning of cell-containing droplets. We have demonstrated that an on-demand patterning of cells over a flat surface is feasible with precise control of cell number at each deposition. Most notably, the potential to draw intricate patterns with arrays of multiple cell types and density gradients is a promising feature of inkjet bioprinting that would be unmatched by other methods. Bicolor arrays have been successfully printed in the present study to test the principle, and even more complex pattern designs could be achieved should the need arise. Our unique combination of cell-printing printheads and industrial printheads also enabled us to develop multilayered structures by association with hydrogel biomaterials, with a controlled thickness down to only a dozen micrometers between each layer. Various strategies for layer-by-layer cell deposition have been attempted previously^{21,22}); but to the best of our knowledge, this is the first report of such finely stratified cellular constructs developed entirely based on an inkjet system. One ultimate goal would be to achieve true drop-on-demand printing at the single-cell resolution, which would signal the potential for novel approaches to the reconstruction and exploration of the complexity of tissue

microenvironments in synergy with the recent rapid advances in single cell analysis.

Despite considerable progress, our technology still faces several limitations that are yet to be resolved. The first issue is that the X-Y surface printing resolution decreases when attempting to draw continuous lines or to increase the density of cellular deposition. Our lines are generally around 100 μm wide, which is quite thick compared with the high resolution we have achieved on the vertical Z direction. This is essentially due to physical properties such as surface tension of the printed materials that can result in the cells moving away from the droplet impact point before their immobilization. Therefore, further optimization and validation are required by taking into account variable cell size, cell density, and materials used as bioink. Finally, the development of bioink materials is also crucial for improving tissue construction in 3D. To obtain fully functional tissues, hydrogel materials that hold the cells together should not only provide physical support but also be biocompatible and able to promote appropriate cellular growth and maturation²³). In this regard, our method requires fast-gelling materials with rheological properties that are compatible with a stable ejection from the inkjet printhead while ensuring precise deposition and rapid immobilization of cells into layers. We are currently using alginate hydrogel as the material of choice since both its precursor and its cross-linking agent (calcium chloride) can be inkjet-printed and provide adequate mechanical strength by forming a solid scaffold layer on contact. However, alginate is not often appropriate for long-term culture since it lacks the cell-adhesive properties required for the cells to interact and function properly¹⁷). Investigations on more suitable materials are underway to provide cellular environments closer to native ECM, including the use of modified alginate, or blending with other cell-adhesive and biodegradable polymers such as fibrin and gelatin²⁴).

5. Conclusions

In this work, we have demonstrated that inkjet bioprinting has the potential to become one of the most powerful technologies for precise tissue construction. Our experience in industrial printing enabled us to address each challenge with systematic engineering solutions. First, we developed an innovative printhead specifically designed to eject living cell suspensions and optimized the printing conditions for reliable dispensing and cell survival. In addition, we built a multi-ink bioprinting system to demonstrate that cells and materials can be effectively arranged in both 2D high-precision patterns and 3D multilayered constructs in a unique manner. Mechanical refinements and biomaterial development are still required to improve the patterning resolution and 3D tissue formation. However, inkjet bioprinting could evolve into a versatile system for the production of structurally organized multicomponent constructs tailored to meet the requirements of various applications such as regenerative medicine, *in vitro* testing, or disease modeling.

References

- 1) K. Takahashi et al.: Induction of Pluripotent Stem Cells from Adult Human Fibroblasts by Defined Factors, *Cell*, Vol. 131, No. 5, pp. 861–872 (2007).
- 2) J. Groll et al.: Biofabrication: Reappraising the Definition in an Evolving Field, *Biofabrication*, Vol. 8, No. 1, pp. 13001–13006 (2016).
- 3) S.V. Murphy, A. Atala: 3D Bioprinting of Tissues and Organs, *Nat. Biotechnol.*, Vol. 32, No. 8, pp. 773–785 (2014).
- 4) A. Arslan-Yildiz et al.: Towards Artificial Tissue Models: Past, Present, and Future of 3D Bioprinting, *Biofabrication*, Vol. 8, No. 1, p. 14103 (2016).
- 5) H. Gudupati, M. Dey, I. Ozbolat: A Comprehensive Review on Droplet-based Bioprinting: Past, Present and Future, *Biomaterials*, Vol. 102, pp. 20–42 (2016).
- 6) B. Derby: Bioprinting: Inkjet Printing Proteins and Hybrid Cell-containing Materials and Structures, *J. Mater. Chem.*, Vol. 18, No. 47, pp. 5717–5721 (2008).
- 7) T. Xu et al.: Inkjet Printing of Viable Mammalian Cells, *Biomaterials*, Vol. 26, No. 1, pp. 93–99 (2005).
- 8) M. Nakamura et al.: Biocompatible Inkjet Printing Technique for Designed Seeding of Individual Living Cells, *Tissue Eng.*, Vol. 11, No. 11–12, pp. 1658–1666 (2005).
- 9) R. E. Saunders, J. E. Gough, B. Derby: Delivery of Human Fibroblast Cells by Piezoelectric Drop-on-demand Inkjet Printing, *Biomaterials*, Vol. 29, No. 2, pp. 193–203 (2008).
- 10) A. Gross et al.: Single-cell Printer: Automated, on Demand, and Label Free, *J. Lab. Autom.*, Vol. 18, No. 6, pp. 504–518 (2013).
- 11) E. Cheng et al.: Investigation of the Hydrodynamic Response of Cells in Drop on Demand Piezoelectric Inkjet Nozzles, *Biofabrication*, Vol. 8, No. 1, p. 15008 (2016).
- 12) C. L. Herran, Y. Huang, W. Chai: Performance Evaluation of Bipolar and Tripolar Excitations During Nozzle-jetting-based Alginate Microsphere Fabrication, *J. Micromech. Microeng.*, Vol. 22, No. 8, p. 85025 (2012).
- 13) Y. K. Kim et al.: Drop-on-demand Inkjet-based Cell Printing with 30- μ m Nozzle Diameter for Cell-level Accuracy, *Biomicrofluidics*, Vol. 10, No. 6, p. 064110 (2016).
- 14) K. Arai et al.: Three-dimensional Inkjet Biofabrication Based on Designed Images, *Biofabrication*, Vol. 3, No. 3, p. 34113 (2011).
- 15) X. Cui, T. Boland: Human Microvasculature Fabrication using Thermal Inkjet Printing Technology, *Biomaterials*, Vol. 30, No. 31, pp. 6221–6227 (2009).

- 16) A. Faulkner-Jones et al.: Bioprinting of Human Pluripotent Stem Cells and their Directed Differentiation into Hepatocyte-like Cells for the Generation of Mini-livers in 3D, *Biofabrication*, Vol. 7, No. 4, p. 44102 (2015).
- 17) M. Nakamura et al.: Biomatrices and Biomaterials for Future Developments of Bioprinting and Biofabrication, *Biofabrication*, Vol. 2, No. 1, p. 14110 (2010).
- 18) G. Perçin, B. T. Khuri-Yakub: Piezoelectric Droplet Ejector for Ink-jet Printing of Fluids and Solid Particles, *Rev. Sci. Instrum.*, Vol. 74, No. 2, pp. 1120–1127 (2003).
- 19) Z. Zhang et al.: Printing-induced Cell Injury Evaluation During Laser Printing of 3T3 Mouse Fibroblasts, *Biofabrication*, Vol. 9, No. 2, p. 25038 (2017).
- 20) W. Hu, C. Berdugo, J. J. Chalmers: The Potential of Hydrodynamic Damage to Animal Cells of Industrial Relevance: Current Understanding, *Cytotechnology*, Vol. 63, No. 5, pp. 445–460 (2011).
- 21) S. Moon et al.: Layer by Layer Three-dimensional Tissue Epitaxy by Cell-laden Hydrogel Droplets, *Tissue Eng. Part C Methods*, Vol. 16, No. 1, pp. 157–166 (2010).
- 22) L. Koch et al.: Skin Tissue Generation by Laser Cell Printing, *Biotechnol. Bioeng.*, Vol. 109, No. 7, pp. 1855–1863 (2012).
- 23) J. Malda et al.: 25th Anniversary Article: Engineering Hydrogels for Biofabrication, *Adv. Mater.*, Vol. 25, No. 36, pp. 5011–5028 (2013).
- 24) T. Jungst et al.: Strategies and Molecular Design Criteria for 3D Printable Hydrogels, *Chem. Rev.*, Vol. 116, No. 3, pp. 1496–1539 (2016).